Tumor-infiltrating regulatory T lymphocytes orchestrate oncogenic PAK1-conferred immune evasion in clear-cell renal cell carcinoma

Yang Qu
Zhongshan Hospital Fudan University
Jiajun Wang
Zhongshan Hospital Fudan University
Qi Bai
Zhongshan Hospital Fudan University
Yangyang Qi
Fudan University School of Basic Medical Sciences
Yifan Chen
Fudan University School of Basic Medical Sciences
Lingli Chen
Zhongshan Hospital Fudan University
Peipei Zhang
Shanghai Jiao Tong University Medical School Affiliated Ruijin Hospital
Zewei Wang
Zhongshan Hospital Fudan University
Zhiyuan Lin
Zhongshan Hospital Fudan University
Ying Xiong
Zhongshan Hospital Fudan University
Yu Xia
Zhongshan Hospital Fudan University
Weijuan Zhang
Fudan University School of Basic Medical Sciences
Yuanfeng Yang
Zhongshan Hospital Fudan University
Li Liu
Zhongshan Hospital Fudan University
Jianming Guo
Zhongshan Hospital Fudan University
Jiejie Xu (jjxufdu@fudan.edu.cn)

Fudan University https://orcid.org/0000-0001-7431-9063

Research article

Keywords: Clear-cell renal cell carcinoma, PAK1, Tumor-infiltrating regulatory T lymphocytes, Immune evasion, CCL22

Posted Date: August 30th, 2019

DOI: https://doi.org/10.21203/rs.2.13684/v1

Version of Record: A version of this preprint was published at European Urology Supplements on March 1st, 2019. See the published version at https://doi.org/10.1016/S1569-9056(19)30065-X.

Abstract

Background: Little is known about the associations between PAK1 and anti-tumor immunity in clear-cell renal cell carcinoma (ccRCC). This study aims to explore the prognostic value of PAK1 in ccRCC patients and investigated the molecular immune mechanism for its oncogenic role. Methods: We retrospectively enrolled 282 ccRCC patients undergoing nephrectomy between 2005 and 2007 in Zhongshan hospital. Immunohistochemistry evaluated PAK1, CCL22, FOXP3 and CD8 expression in clinical specimens. Fresh tumor tissues, para-tumor tissues and peripheral blood samples for RT-PCR, ELISA, flow cytometry analyses were collected from patients who underwent nephrectomy in Zhongshan Hospital from September 2017 to April 2018. We compared clinical outcomes by Kaplan-Meier survival analysis and Cox regression model. Bioinformatics analysis performed in TCGA KIRC cohort. Results: High PAK1 expression indicated poorer overall survival (OS) and recurrence free survival (RFS) (both $p<0.001$) in ccRCC patients. Multivariate analyses indicated PAK1 as an independent prognostic factor. In clinical samples, PAK1 clearly correlated with immunosuppressive microenvironment in ccRCC tissues. Significantly, PAK1 positively correlated with Tumor-infiltrating regulatory T lymphocytes (Tregs). Furthermore, IL-10+ and TGF-β+ tumor-infiltrating Tregs both increased in PAK1 high tumors. Additionally, CCL22 was highly secreted in PAK1 high tumors. After treated by IPA-3 (an PAK1 inhibitor), CCL22 secretion was clearly inhibited ($p<0.001$). Finally, we built a nomogram to predict overall survival for ccRCC patients with higher predictive accuracy. Conclusions: Increased PAK1 expression predicted dismal prognosis in ccRCC patients by inducing tumor immune escape. IL-10+ and TGF-β+ tumor-infiltrating Tregs recruited by CCL22 play dominant immunosuppressive roles in PAK1 high tumors.

Background

Renal cell carcinoma (RCC) is the 7^{th} most common cancer in human beings [1] and clear-cell renal cell carcinoma (ccRCC) is the commonest one accounting for more than 80% cases [2]. Despite huge progresses in diagnosis and management, RCC shows a dismal prognosis and estimates 14970 deaths in the USA in 2018 [3], especially for the patients with a metastatic RCC (mRCC). Because RCC patients are insensitive to radiotherapy and chemotherapy, tyrosine kinase inhibitors (TKIs) have been approved for first-line treatment in mRCC since last decade. However, many patients still get disease progression after TKIs therapy owing to drug resistance. In the past few years, PD−1 inhibitors have been approved by the FDA for targeted therapy of ccRCC patients, indicating the therapeutic potential of immune inhibitors. Additionally, due to the heterogeneity of molecular phenotype, classical prognostic models, such as TNM stage, the Mayo clinic stage, size, grade, and necrosis score (SSIGN) [4] and the University of Los Angeles integrated staging system (UISS) [5] category systems, have limited prognostic value. Therefore, effective therapeutic and prognostic factors are still in great need for RCC patients.

It is worth noting that RCC represents a highly immunosensitive tumor due to the high levels of tumor infiltrating immune cells [6]. Tumor microenvironment (TME) plays an important role in different tumors. Our recent researches have showed the fundamental role of TME in RCC and gastric cancer [7,8]. Tumor-infiltrating lymphocytes (TILs) are of great importance in TME. Influenced by cellular and soluble

components, TILs are divided into multiple subtypes and play complex roles in tumor development [9]. Thus, TILs can demonstrate either tumor-suppressive or tumor-promoting effects. For instance, regulatory T cells (Tregs) are associated with pro-tumor functions in RCC [10]. Tregs can inhibit the activation and proliferation of $CD4^+$ T cells and $CD8^+$ T cells through different ways [11]. Additionally, tumor-infiltrating Tregs are found to traffic to tumorous from peripheral blood under the influence of CC-chemokine ligand 22 (CCL22) [12].

The p21-activated kinases (Paks), a family of serine/threonine kinases, have been found to be key regulators of cancer-cell signaling networks [13]. As the best-characterized member of Paks family, PAK1 was identified as a protein that interacts with Cdc 42 and Rho-like G proteins. Activated by Rho-GTPases, PAK1 acts as a downstream activator for various oncogenic signaling pathways [14]. As an oncogene, PAK1 was reported to be associated with pancreatic cancer [15], gastric cancer [16] and colorectal cancer [17]. In previous study, we revealed the vital effects of PAK1 in non-metastatic RCC [18] and in hepatoma [19]. However, few studies focused on PAK1 in TME. Interestingly, Watt J et al found that PAK1 could interrupt tumor-associated immunocytes through activating NF-κB [20]. Therefore, we investigated the oncogenic role of PAK1 via tumor immunomodulation in ccRCC patients.

Our research provided direct evidence that tumoral PAK1, which correlated with survival, induced immune escape in ccRCC patients. We found $IL-10^+$ and $TGF-\beta^+$ tumor-infiltrating Tregs recruited by CCL22 play dominant immunosuppressive roles in $PAK1^{high}$ tumors.

Methods

Patients

Three independent cohorts of ccRCC patients were enrolled in our study. Zhongshan cohort retrospectively enrolled 282 ccRCC patients who underwent nephrectomy at the Department of Urology, Zhongshan Hospital, Fudan University between Jan 2005 and Jun 2007. Patients with former malignant tumors, perioperative mortalities or multi-primary cancers were excluded. The last follow up time was Jan 1, 2018 with a median follow-up of 115 months. We also enrolled 30 ccRCC patients who underwent nephrectomy in Zhongshan Hospital from September 2017 to April 2018 and named this cohort as Fresh Clinical Sample (FCS) cohort. Fresh tumor tissues, para-tumor tissues and peripheral blood for RT-PCR, ELISA and flowcytometry analyses were get from FCS cohort. Our study was approved by the Clinical Research Ethics Committee of Zhongshan Hospital, Fudan University with the approval number B2015–030.

KIRC cohort comprising 534 ccRCC patients from The Cancer Genome Atlas Kidney Renal Clear Cell Carcinoma cohort, which was downloaded from UCSC Xena. In KIRC cohort, median expression was used to define high/low expression for PAK1 and immune gene signatures. The immune cell compositions were calculated by CIBERSORT [21]. The protein-protein interaction (PPI) network was identified by the STRING database and visualized by Cytoscope [22,23].

Tumor histology and nucleus grade were determined according to the 2004 WHO criteria [24] and the Fuhrman grading system [25]. Each patient was staged with radiographic reports and postoperative pathological results, which were confirmed according to 2010 AJCC TNM classification [26]. The primary outcome, overall survival (OS), was defined as the date of nephrectomy to the time of death or the most recent follow-up. Recurrence free survival (RFS) was calculated from the time of nephrectomy to the time of recurrence, which defined as local or distant metastases confirmed by imaging, biopsy or physical examination.

Tissue microarray and Immunohistochemistry

Tissue microarray construction and the immunohistochemistry (IHC) protocol have been described previously [27]. Mouse monoclonal antibodies for PAK1 (Santa Cruz), CD8 (DAKO), CCL22 (Abcam), FOXP3 (Abcam), CD68 (DAKO), CD66b (BD) and tryptase (Abcam) were used for IHC. Olympus CDD camera, Nikon eclipse Ti-s microscope and NIS-Elements F3.2 software were used to record the results. Three independent shots were obtained in each core.

Two pathologists evaluated the PAK1 staining using a semi-quantitative immunoreactivity score (IRS) algorithm. IRS score was derived from the multiplication of intensity of IHC staining (0, negative; 1, weak; 2, intermediate; and 3, strong) and percentage of positive tumor cells (1 point for each 10% increment). Both cores were examined and the mean IRS score was calculated. In case of disagreement, the slides were reviewed by two observers until a consensus was reached. CCL22 staining was evaluated by IOD score described previously [28]. Immune cells densities were converted from the total positive cells in each core. The cutoff value was determined by X-tile 3.6.1 (Yale University).

Flow cytometry

For fresh tumor tissues and para-tumor tissues, single cells were isolated by collagenase overnight. These cells stained with appropriate monoclonal antibodies for 30 minutes at 4°C. Fluorochrome-conjugated antibodies specific for human CD45, CD8, IFNG, GZMB, CD4, CD25, FOXP3, IL−10, TGFB, CD16, CD56 (BD) were used. Stained cells were washed, re-suspended in PBS. Flow cytometry was performed using BDcelesta and analyzed by FlowJo software.

ELISA

The concentrations of CCL22 were measured by ELISA in supernatants of tumor tissue or blood serum samples which were collected from proper conditioned media. All 30 cases of ccRCC tissue were additionally treated with PAK1 inhibitor IPA−3 (7.5 μM) for 24 hours as described previously [18]. ELISA were performed using human MDC ELISA kit (Abcam) according to the instructions.

Real-time PCR with reverse transcription

Total RNA from clinical specimens was extracted using TRIzol reagent (Invitrogen) according to the instructions. Reverse transcription was performed by QuantiTect reverse transcription kits (QIAGEN). Primers used: PAK1 primers: AGTTTCAGAAGATGAGGATGATGA and AATCACAGACCG- TGTGTATACAG; GADPH primers: AAGGTCGGAGTCAACGGATT and TGGTGGCTGGAAGATGTTTGTC. The mRNA level of PAK1 was normalized by GADPH.

Statistical analyses

Statistical analysis in our study was performed by SPSS, GraphPad Prism, MedCalc, Funrich, X-tile, Stata and R software with the “rms”, “ggplot” and “smoothHR” packages. Cut-off point for the high/low definition of PAK1 expression was determined at IRS score 9.9 using X-tile software and checked by smooth HR curves. Data was censored until the last follow up time or the time when patient died. The connections between the PAK1 expression and baseline characteristics were evaluated by χ^2 test, Fisher’s exact method or Cochran-Mantel-Haenszel χ^2 test. Impacts of PAK1 on prognosis were assessed by Kaplan–Meier method and log-rank test. Univariate and multivariate analyses were done with the Cox proportional hazards regression tests. The differences between two groups were analyzed by Student’s t-test, paired t-test or Mann-Whitney U test. Correlations between two parameters were determined using Spearman’s correlation. Gene set enrichment analyses (GSEA) were carried out with FDR<0.25 and P value < 0.05 [29]. Gene sets were downloaded from the Broad Institute’s MSigDB. A two-tailed P value of less than 0.05 was considered statistically significant.

Results

Increased tumoral PAK1 expression correlates with poor prognosis and immune escape in ccRCC patients

We evaluated the PAK1 expression by IHC staining in all 282 patients’ tissue microarrays. PAK1 was predominantly expressed in the nucleus and membrane of tumor cells (Figure 1A). The IRS distributions of PAK1 were 3.2–28.6. Based on minimum *p* value method, we defined the cut-off point as 9.9 and checked with the smooth HR curve (Figure 1B), which showed a significant prognostic difference between the high and low PAK1 expression groups.

Patients’ baseline characteristics and the association of those clinicopathological variables with PAK1 were summarized in Table S1. With the cut-off point of 9.9, 143 (50.7%) patients were defined as PAK1 low expression and 139 (49.3%) patients with a high expression level. PAK1 was positively correlated with TNM stage in Zhongshan cohort and KIRC cohort (Figure 1C). Additionally, high PAK1 expression was found associated with poorer OS and RFS (Figure 1D, both $p<0.001$). Multivariate analysis showed PAK1 as an independent prognostic predictor for OS ($p = 0.018$) and RFS ($p = 0.003$) (Table S2).

To explore the mechanism of PAK1 in tumor progress, we firstly performed clustering analysis in KIRC cohort. GO analysis using top 500 differentially expressed genes was performed between high/low PAK1 groups. Obviously, immune response is the most enriched biological process (Figure 1E). Additionally, PAK1 has a positive correlation with most immunosuppressive genes as well as negatively correlates with most immune-killing genes (Figure 1F). These results indicated that PAK1 might contribute to immunosuppressive tumor environment and immune escape in ccRCC patients. We further investigated this phenomenon using clinical samples. As presented in Figure 1G, $PAK1^{high}$ tumors were infiltrated with significantly decreased $CD8^+$ T cells. Moreover, the function of $CD8^+$ T cells was impaired as IFN-γ^+ $CD8^+$ T cells and NK cells frequencies were decreased in $PAK1^{high}$ group (Figure H). Similarly, $GZMB^+$ $CD8^+$ T cells and NK cells tended to decrease in $PAK1^{high}$ tumor (Figure I). Thus, we found PAK1 contributes to immune escape in ccRCC patients.

Increased tumoral PAK1 correlates with the highly infiltration of Tregs and reduces immunosurveillance in ccRCC patients

To identify which immunomodulatory cell dominantly contributes to the immune escape induced by PAK1, we evaluated different immune-regulatory cells by IHC in Zhongshan cohort (Figure 2A). Based on our databases, Tregs were significantly infiltrated in $PAK1^{high}$ tumors, while the infiltration of macrophages, neutrophils and mast cells had no statistical significance between high/low PAK1 groups (Figure 2B). Tregs had a strong positive correlation with PAK1 expression (Figure 2B, $r = 0.579$, $p<0.001$). Moreover, the mRNA levels of FOXP3 were also increased in $PAK1^{high}$ tumors in KIRC cohort (Figure 2C). Additionally, flow cytometry showed the infiltration of Tregs clearly increased in ccRCC tissue relative to para-ccRCC tissue (Figure 2D). The frequencies of Tregs also significantly elevated in $PAK1^{high}$ tumor tissues (Figure 2E).

Obviously, $CD8^+$ T cells / Tregs ratio (CD8/Treg ratio) significantly decreased in $PAK1^{high}$ tumor tissues (Figure 2F). We identified some differentially expressed genes in tumors with low CD8/Treg ratio versus tumors with high CD8/Treg ratio in volcano plot (Figure 2G). Genes related to $CD8^+$ T cells (CD8A, CD8B, CD27, CD3G), cytotoxicity (IFNG, GZMK, GZMA, KLRK1) and immune-control chemokine (CXCL9–11, CXCL13) were among the top 50 down-regulated genes. We further performed PPI analysis with top 100 down-regulated genes in low CD8/Treg ratio group. Genes related to anti-tumor immunity (IFNG, CD8A, CCL5, GZMA, CD27, CD3D, CCR5, PRF1, CD3E, CXCR3, FASLG) were in center of PPI network (Figure 2H). These results showed PAK1 has a positive correlation with Tregs, which correlates to down-regulation of cytotoxic effect in ccRCC patients.

IL–10^{+} and TGF-β^{+} Tregs dominate immunosuppression in PAK1^{high} ccRCC tissue

We further performed Gene set enrichment analysis (GSEA) to explore the difference between low CD8/Treg ratio verses high CD8/Treg ratio tumors. We detected 4 main pathway distributions and found most of the significant pathways for down-regulated gene sets were associated with immune surveillance (Figure 3A). We highlighted the top 24 immune-related pathways in Figure 3B-C (all FDR<0.1 and NES>1.6). Moreover, we found an enhancement of IL–10^{+} and TGF-β^{+} Tregs frequencies in ccRCC tissues relative to para-ccRCC tissues (Figure 3D), hinting that IL–10 and TGF-β secreted by Tregs dominated this immunosuppressive microenvironment. Additionally, IL–10^{+} and TGF-β^{+} Tregs frequencies also significantly increased in PAK1^{high} tumors (Figure 3E). These results indicated that PAK1 contributed to the activation of Tregs, which further inhibited anti-tumor immunity in ccRCC patients.

Increased tumoral PAK1 induces CCL22 secretion in ccRCC tissue

We further investigated the potential chemokine regulating infiltration of Tregs in PAK1^{high} tumors. Heatmap showed the relative mRNA levels of 36 chemokines in 534 ccRCC patients based on KIRC cohort (Figure 4A).Significance Analysis for Microarray (SAM) identified CCL22, CCL25 and CCL17 (delta value>2) that highly increased in the PAK1^{high} patients (Figure 4A). Volcano plot also showed CCL22 highly expressed in PAK1^{high} tumors (Figure 4B, logFC = 0.519, -log10p = 4.911). We further performed IHC staining (Figure 4C) and ELISA to evaluate CCL22 in clinical samples. PAK1 had a strong positive correlation with CCL22 both in KIRC cohort and Zhongshan cohort (Figure 4D). In FCS cohort, CCL22 concentrations both increased in PAK1^{high} ccRCC tissues and PAK1^{high} peripheral blood samples (Figure 4E).

To further ensure that PAK1 could induce immunosuppressive TME via secreting CCL22, we added IPA–3 to tumor suspension and detected the concentration of CCL22 after treated for 24 hours. The concentration of CCL22 decreased in IPA–3 treatment group with a strong statistical significance (Figure 4F). These findings suggest blocking PAK1 pathway may promote anti-tumor immunity by exhibiting CCL22 secretion.

CCL22 promotes immunosuppression by recruiting IL–10+ and TGF-β+ Tregs in ccRCC patients

According to KIRC cohort, CCL22 plays a major role in recruiting Tregs (Figure 5A). Furthermore, CCL22 and its receptor CCR5 were highly up-regulated in PAK1^{high} tumors (Figure 5B). In this study, CCL22 had a strong positive correlation with PAK1 based on all three cohorts (Figure 5C-E). Moreover, the infiltration of

IL−10^{+} and TGF-β^{+} Tregs was obviously enhanced in CCL22^{high} tumors (Figure 5F). This indicated that CCL22-CCR5 pathway might contribute to the activation of Tregs.

PAK1-CCL22-Tregs axis interlinks prognosis of ccRCC patients

VENN diagram showed the consistency of PAK1-CCL22-Tregs axis (Figure 6A). Furthermore, we verify the correlation among PAK1-CCL22-FOXP3 in 17 different TCGA cancer cohorts. Interestingly, this axis shows favorable consistency in most urological malignancies (KIRC, KICH, KIRP, UCS, PRAD and TGCT). Additionally, we found high expression of CCL22 and FOXP3 also predict dismal prognosis for ccRCC patients (Figure 6C). Finally, we built a PAK1-based nomogram for clinical usage (Figure 6D). It is excited to see our nomogram do better predictive jobs than existed prognostic models (Table S3). A potential schematic model was presented in Figure S1.

Discussion

In our study, we accessed the prognostic value of PAK1 expression level in ccRCC patients. Then, we used clinical samples and public databases to investigate the tumor-promoting effects of PAK1 via regulating immunosurveillance.

Our study confirmed PAK1 as an independent prognostic predictor for ccRCC patients according to univariate and multivariate analysis. High PAK1 expression was associated with poorer OS and RFS. Furthermore, CD8^{+} T cells infiltration clearly decreased in PAK1^{high} tumors. In the meanwhile, IFN-γ^{+} and GZMB^{+} CD8^{+} T cells fraction also decreased in PAK1^{high} tumors. Therefore, PAK1 contributed to tumor immune escape by inhibiting immune-killing function. More than that, we investigated the subgroups of functional Tregs considering the heterogeneity. Based on our results, IL−10^{+} and TGF-β^{+} tumor-infiltrating Tregs play dominant immunosuppressive roles in PAK1^{high} tumors.

We further tried to figure out which chemokine contributes to the recruitment of Tregs in PAK1^{high} tumors. Based on the bioinformatic analysis of KIRC cohort, the mRNA level of CCL22 was obviously increased in PAK1^{high} tumors. This increase of CCL22 was also verified by our clinical samples. Moreover, CCL22 was positively correlated with IL−10^{+} and TGF-β^{+} Tregs, which played an important role in PAK1-mediated tumor progression. Most importantly, we demonstrated that PAK1 inhibitor could inhibit the secretion of CCL22 in ccRCC tissue. All these findings imply that PAK1 contributes to tumor progression via inducing immunosuppressive microenvironment by promoting to the recruitment of Tregs.

RCC is highly immunologically sensitive with many immunocytes infiltrated. Hakimi et al divided RCC into three types according to the infiltration of immune cells and found they were related to the prognosis and drug responsiveness [30]. Our study firstly reported the interaction between tumoral PAK1 and anti-tumor

immunity in ccRCC. We found that PAK1^{high} ccRCC promotes its progression by inducing immune escape. IL−10^{+} and TGF-β^{+} Tregs recruited by CCL22 play a key role in this process.

As a well-known immunomodulatory cell, Treg cell shows an immunosuppressive effect and correlates with poor prognosis in many cancers [31,32]. Tregs have three major ways to inhibit anti-tumor immunity: secreting inhibitory cytokines, contacting with T cells directly and expressing costimulatory molecules like CTLA4 [33]. Our study shows PAK1 might promote Tregs to secret IL−10 and TGF-β, which dominantly inhibited anti-tumor immunity in PAK1^{high} tumors.

Tumor immunotherapy has become a new hot spot with the large-scale research and development of immune checkpoint inhibitors. In the latest EAU guideline, nivolumab and cabozantinib have been recommended as second-line treatments for mRCC [34]. However, the efficacy of immune checkpoint inhibitors is still limited as the median OS is only 25 months [35]. Therefore, we hope to find a molecular target that limits the efficacy of immunotherapy and improve the efficacy by intervening on this target. Our research found PAK1 as a promising target to improve drug responsiveness. Inhibiting PAK1 can theoretically remove the immunosuppressive microenvironment and enhance the anti-tumor immune effects. Thus, we hope future studies can evaluate the efficacy of combined therapy of PAK1 inhibitors and immune checkpoint inhibitors.

Some limitations of this study need to be acknowledged. The major one is the relatively small sample size which was obtained from one single institution. This results in boundary p-values in some analyses. External validations are still required. The second one is the retrospective design which requires prospective studies to further verify the results.

Conclusion

In conclusion, using clinical ccRCC samples and public database, our study suggested that high PAK1 expression predicted dismal prognosis in ccRCC patients by inducing tumor immune escape. IL−10^{+} and TGF-β^{+} tumor-infiltrating Tregs recruited by CCL22 play a dominant immunosuppressive role in PAK1^{high} tumors. Immune checkpoint blocker combined with PAK1 inhibitor might have potential treatment benefits in ccRCC patients.

List Of Abbreviations

ccRCC：clear-cell renal cell carcinoma；

TCGA：The Cancer Genome Atlas；

OS： overall survival；

RFS：recurrence free survival；

Tregs：regulatory T lymphocytes；

RCC：renal cell carcinoma；

mRCC：metastatic renal cell carcinoma；

TKIs：tyrosine kinase inhibitors；

SSIGN：stage, size, grade, and necrosis score；

UISS：University of Los Angeles integrated staging system；

TME：tumor microenvironment；

TILs：tumor-infiltrating lymphocytes；

CCL22：CC-chemokine ligand 22；

Paks：the p21-activated kinases；

PPI：protein-protein interaction；

IHC： immunohistochemistry；

IRS：immunoreactivity score；

GSEA： gene set enrichment analyses.

Declarations

Ethics approval and consent to participate

Our study was approved by the Clinical Research Ethics Committee of Zhongshan Hospital, Fudan University with the approval number B2015–030.

Consent for publication

Each patient in cohort was informed consent.

Availability of data and materials

The datasets used and/or analysed during the current study are available from the corresponding author on reasonable request.

Competing interest

The authors declare no conflict of interest.

Funding

This work was supported by grants from National Natural Science Foundation of China (81472227, 81472376, 31770851, 81702496, 81702497, 81702805, 81772696), Shanghai Municipal Natural Science Foundation (17ZR1405100), Shanghai Sailing Program (19YF1407900), Shanghai Municipal Commission of Health and Family Planning (20174Y0042) and Zhongshan Hospital Science Foundation (2016ZSQN30, 2017ZSQN18, 2017ZSYQ26). All these study sponsors have no roles in design of the study or collection, analysis, and interpretation of data.

Author contributions

Y. Qu, J. Wang and Q. Bai for acquisition of data, analysis and interpretation of data, statistical analysis and drafting of the manuscript; Y. Qi, Y. Chen, L. Chen, P. Zhang, Z. Wang, Z. Lin, Y. Xiong, Y. Xia, W. Zhang and Y. Yang for technical and material support; L. Liu, J. Guo and J. Xu for study concept and design, analysis and interpretation of data, drafting of the manuscript, obtained funding and study supervision. All authors read and approved the final manuscript.

Acknowledgements

Not applicable.

References

1.Escudier B., Porta C., Schmidinger M., Rioux-Leclercq N., Bex A., Khoo V., et al. Renal cell carcinoma: ESMO Clinical Practice Guidelines for diagnosis, treatment and follow-up. ANN ONCOL 2016;27: v58–68.

2.Rini B. I., Campbell S. C., Escudier B. Renal cell carcinoma. LANCET 2009;373: 1119–32.

3.Siegel R. L., Miller K. D., Jemal A. Cancer statistics, 2018. CA Cancer J Clin 2018;68: 7–30.

4.Frank I., Blute M. L., Cheville J. C., Lohse C. M., Weaver A. L., Zincke H. An outcome prediction model for patients with clear cell renal cell carcinoma treated with radical nephrectomy based on tumor stage, size, grade and necrosis: the SSIGN score. J Urol 2002;168: 2395–400.

5.Leibovich B.C., Blute M. L., Cheville J. C., Lohse C. M., Frank I., Kwon E. D., et al. Prediction of progression after radical nephrectomy for patients with clear cell renal cell carcinoma: a stratification tool for prospective clinical trials. CANCER-AM CANCER SOC 2003;97: 1663–71.

6.Geissler K., Fornara P., Lautenschlager C., Holzhausen H. J., Seliger B., Riemann D. Immune signature of tumor infiltrating immune cells in renal cancer. ONCOIMMUNOLOGY 2015;4: e985082.

7.Fu Q., Xu L., Wang Y., Jiang Q., Liu Z., Zhang J., et al. Tumor-associated macrophage-derived interleukin–23 interlinks kidney cancer glutamine addiction with immune evasion. Eur. Urol. 10.1016/j.eururo.2018.09.030 [Epub ahead of print].

8.Lin C., He H., Liu H., Li R., Chen Y., Qi Y., et al. Tumour-associated macrophages-derived CXCL8 determines immune evasion through autonomous PD-L1 expression in gastric cancer. GUT. 10.1136/gutjnl–2018–316324. [Epub ahead of print].

9.Whiteside T. L. Immune suppression in cancer: effects on immune cells, mechanisms and future therapeutic intervention. SEMIN CANCER BIOL 2006;16: 3–15.

10.Komohara Y., Hasita H., Ohnishi K., Fujiwara Y., Suzu S., Eto M., et al. Macrophage infiltration and its prognostic relevance in clear cell renal cell carcinoma. CANCER SCI 2011;102: 1424–31.

11.Maj T., Wang W., Crespo J., Zhang H., Wang W., Wei S., et al. Oxidative stress controls regulatory T cell apoptosis and suppressor activity and PD-L1-blockade resistance in tumor. NAT IMMUNOL 2017;18: 1332–41.

12.Curiel T. J., Coukos G., Zou L., Alvarez X., Cheng P., Mottram P., et al. Specific recruitment of regulatory T cells in ovarian carcinoma fosters immune privilege and predicts reduced survival. NAT MED 2004;10: 942–9.

13.Keen N., Taylor S. Aurora-kinase inhibitors as anticancer agents. NAT REV CANCER 2004;4: 927–36.

14.Eswaran J., Li D. Q., Shah A., Kumar R. Molecular pathways: targeting p21-activated kinase 1 signaling in cancer—opportunities, challenges, and limitations. CLIN CANCER RES 2012;18: 3743–9.

15.Jagadeeshan S., Subramanian A., Tentu S., Beesetti S., Singhal M., Raghavan S., et al. P21-activated kinase 1 (Pak1) signaling influences therapeutic outcome in pancreatic cancer. ANN ONCOL 2016;27: 1546–56.

16.Wang G., Zhang Q., Song Y., Wang X., Guo Q., Zhang J., et al. PAK1 regulates RUFY3-mediated gastric cancer cell migration and invasion. CELL DEATH DIS 2015;6: e1682.

17.El-Baba C., Mahadevan V., Fahlbusch F. B., Mohan S. S., Rau T. T., Gali-Muhtasib H., et al. Thymoquinone-induced conformational changes of PAK1 interrupt prosurvival MEK-ERK signaling in colorectal cancer. MOL CANCER 2014;13: 201.

18.Zhu Y., Xu L., An H., Liu W., Wang Z., Xu J. p21-activated kinase 1 predicts recurrence and survival in patients with non-metastatic clear cell renal cell carcinoma. INT J UROL 2015;22: 447–53.

19.Xu J., Liu H., Chen L., Wang S., Zhou L., Yun X., et al. Hepatitis B virus X protein confers resistance of hepatoma cells to anoikis by up-regulating and activating p21-activated kinase 1. GASTROENTEROLOGY 2012;143: 199–212.

20.Watt J., Kocher H. M. The desmoplastic stroma of pancreatic cancer is a barrier to immune cell infiltration. ONCOIMMUNOLOGY 2013;2: e26788.

21.Newman A.M., Liu C. L., Green M. R., Gentles A. J., Feng W., Xu Y., et al. Robust enumeration of cell subsets from tissue expression profiles. NAT METHODS 2015;12: 453–7.

22.Szklarczyk D., Franceschini A., Wyder S., Forslund K., Heller D., Huerta-Cepas J., et al. STRING v10: protein-protein interaction networks, integrated over the tree of life. NUCLEIC ACIDS RES 2015;43: D447–52.

23.Shannon P., Markiel A., Ozier O., Baliga N. S., Wang J. T., Ramage D., et al. Cytoscape: a software environment for integrated models of biomolecular interaction networks. GENOME RES 2003;13: 2498–504.

24.Delahunt B., Srigley J. R., Montironi R., Egevad L. Advances in renal neoplasia: recommendations from the 2012 International Society of Urological Pathology Consensus Conference. UROLOGY 2014;83: 969–74.

25.Fuhrman S. A., Lasky L. C., Limas C. Prognostic significance of morphologic parameters in renal cell carcinoma. AM J SURG PATHOL 1982;6: 655–63.

26.Edge S. B., Compton C. C. The American Joint Committee on Cancer: the 7th edition of the AJCC cancer staging manual and the future of TNM. ANN SURG ONCOL 2010;17: 1471–4.

27.Qu Y., Liu L., Wang J., Xi W., Xia Y., Bai Q., et al. Dot1l expression predicts adverse postoperative prognosis of patients with clear-cell renal cell carcinoma. ONCOTARGET 2016;7: 84775–84.

28.Xia Y., Liu L., Xiong Y., Bai Q., Wang J., Xi W., et al. Podoplanin associates with adverse postoperative prognosis of patients with clear cell renal cell carcinoma. CANCER SCI 2016;107: 1243–9.

29.Subramanian A., Tamayo P., Mootha V. K., Mukherjee S., Ebert B. L., Gillette M. A., et al. Gene set enrichment analysis: a knowledge-based approach for interpreting genome-wide expression profiles. Proc Natl Acad Sci U S A 2005;102: 15545–50.

30.Senbabaoglu Y., Gejman R. S., Winer A. G., Liu M., Van Allen E. M., de Velasco G., et al. Tumor immune microenvironment characterization in clear cell renal cell carcinoma identifies prognostic and immunotherapeutically relevant messenger RNA signatures. GENOME BIOL 2016;17: 231.

31.Bates G. J., Fox S. B., Han C., Leek R. D., Garcia J. F., Harris A. L., et al. Quantification of regulatory T cells enables the identification of high-risk breast cancer patients and those at risk of late relapse. J CLIN

ONCOL 2006;24: 5373–80.

32.Gao Q., Qiu S. J., Fan J., Zhou J., Wang X. Y., Xiao Y. S., et al. Intratumoral balance of regulatory and cytotoxic T cells is associated with prognosis of hepatocellular carcinoma after resection. J CLIN ONCOL 2007;25: 2586–93.

33.Zou W. Regulatory T cells, tumour immunity and immunotherapy. NAT REV IMMUNOL 2006;6: 295–307.

34.Escudier B., Porta C., Schmidinger M., Rioux-Leclercq N., Bex A., Khoo V., et al. Renal cell carcinoma: ESMO Clinical Practice Guidelines for diagnosis, treatment and follow-up. ANN ONCOL 2016;27: v58–68.

35.Motzer R. J., Escudier B., McDermott D. F., George S., Hammers H. J., Srinivas S., et al. Nivolumab versus Everolimus in Advanced Renal-Cell Carcinoma. N Engl J Med 2015;373: 1803–13.

Figures

Figure 1

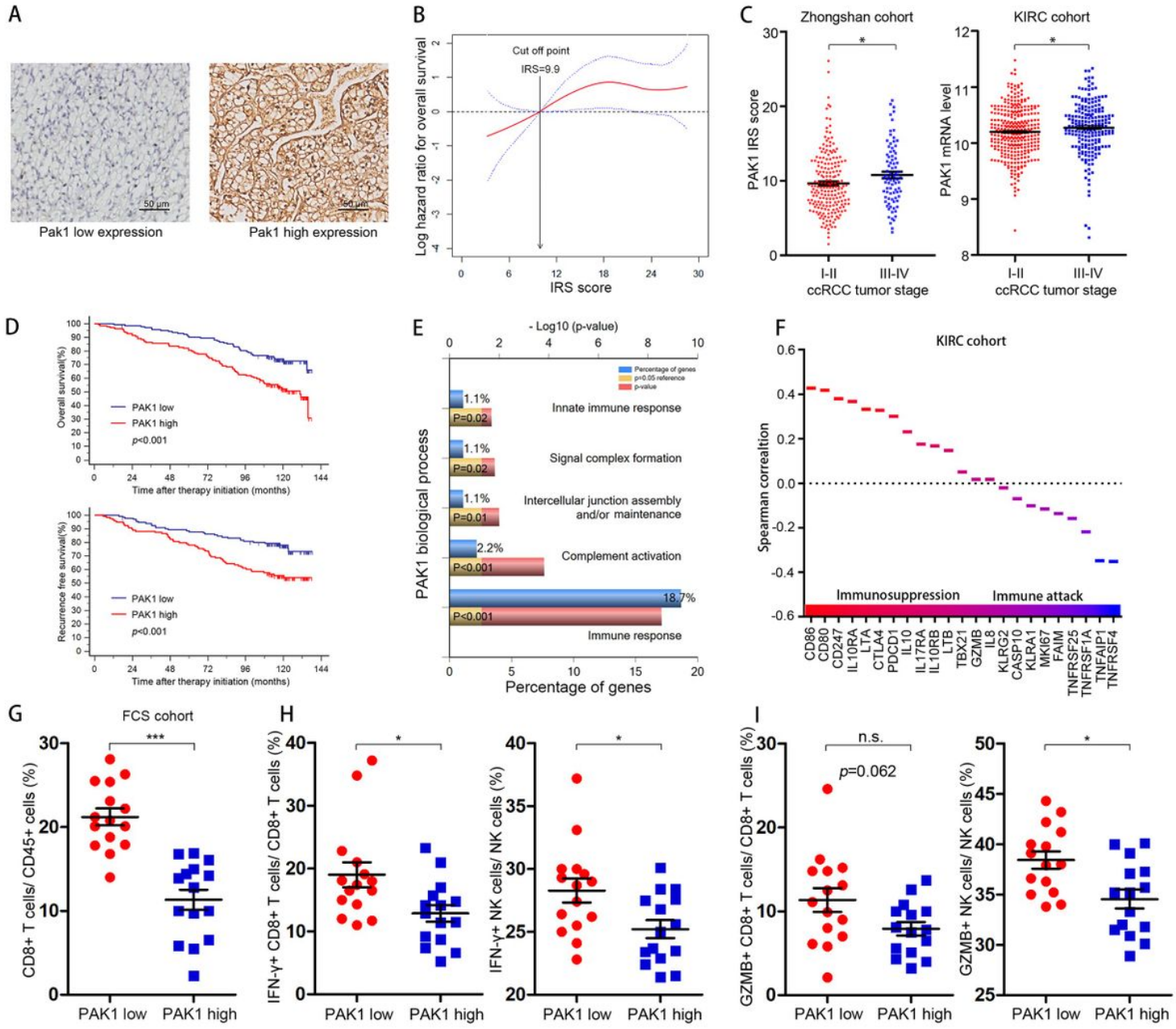

Figure 1

Increased tumoral PAK1 expression correlates with poor prognosis and immune escape in ccRCC patients. (A) Low and high PAK1 expression in ccRCC tissue by IHC in Zhongshan cohort. Scale bar: 50 μm. (B) Smooth estimates of HR (using IRS=9.9 as a reference) show a significant and stable prognostic difference between patients with high/low tumoral PAK1 staining. Dashed lines: 95% confidence bands. (C) PAK1 expression and mRNA level according to TNM stage in Zhongshan cohort and KIRC cohort, respectively. (D) Kaplan-Meier curves comparing OS and RFS in ccRCC patients with high and low PAK1 expression by IHC in Zhongshan cohort. (E) GO analysis performed by top 500 differentially expressed genes between high/low PAK1 expression groups in KIRC cohort. Immune response is the most statistically significant biological process. (F) Waterfall chart of Spearman correlation between PAK1 and

23 immune-associated genes based on KIRC cohort. Red indicates strong positive correlations; blue indicates strong negative correlations. PAK1 has a positive correlation with immunosuppressed genes as well as negatively correlates with most immune killing genes. (G-I) Quantification by flow cytometry of immune cells in ccRCC tissue samples from FCS cohort. (G) CD8+ T cells frequencies of CD45+ leukocytes from patients with PAK1low (n=15) or PAK1high tumors (n=15) are compared. PAK1high tumors are infiltrated with significantly decreased CD8+ T cells. (H) IFN-γ+ or GZMB+ CD8+ T cells frequencies of CD8+ T cells from patients with PAK1low (n=15) or PAK1high tumors (n=15) are compared, respectively. (I) IFN-γ+ or GZMB+ NK cells frequencies of NK cells from patients with PAK1low (n=15) or PAK1high tumors (n=15) are compared, respectively. Bar plots show mean ± SEM. *p<0.05, **p<0.01 and ***p<0.001 for groups connected by horizontal lines.

Figure 2

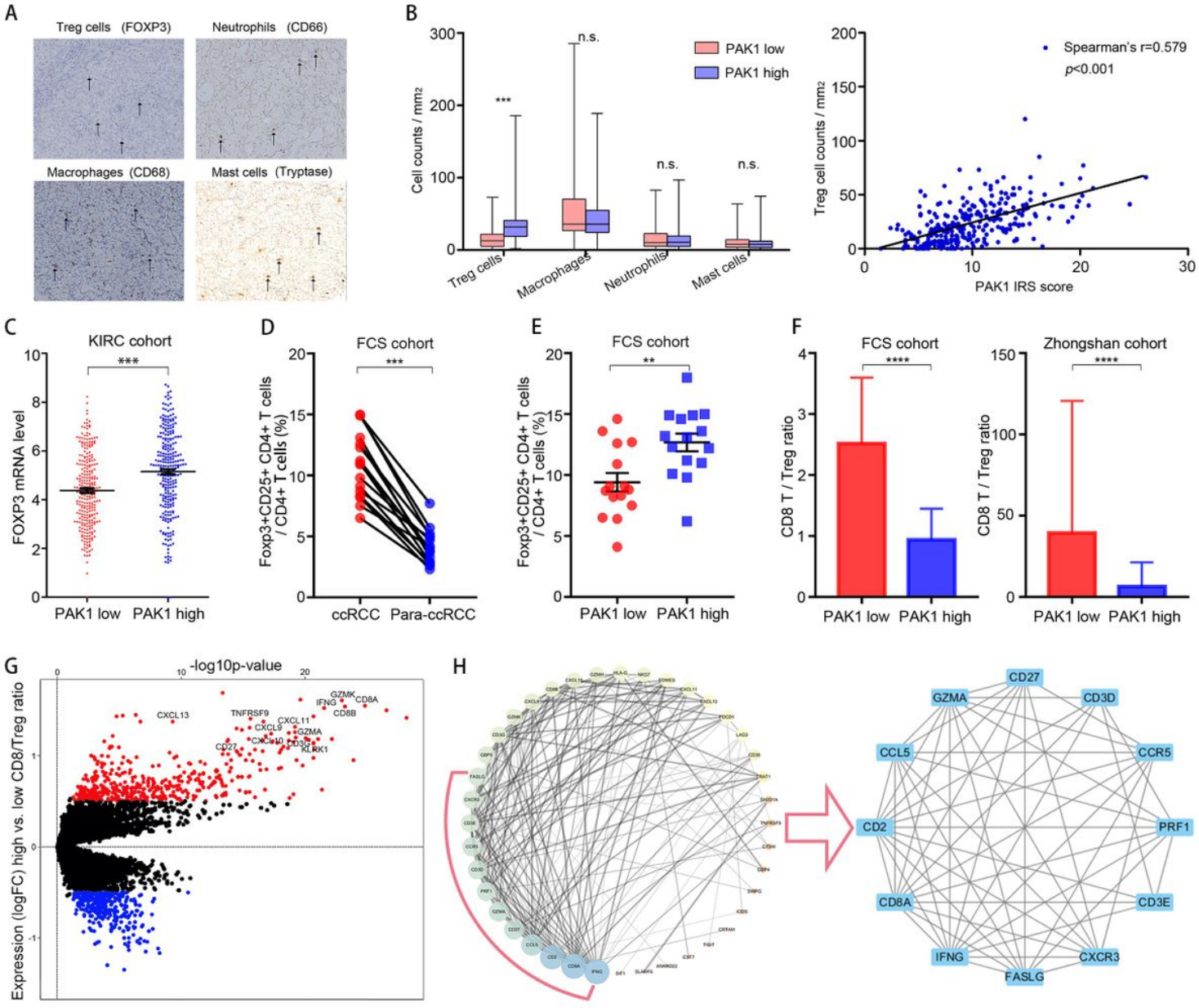

Figure 2

Increased tumoral PAK1 correlates with the highly infiltration of Tregs and reduces immunosurveillance in ccRCC patients. (A) Different immune-regulatory cells (Treg cells, macrophages, neutrophils and mast cells) are evaluated by IHC in Zhongshan cohort. (B) Boxplot compares the counts of different immune-regulatory cells with different PAK1 expression groups measuring by IHC in Zhongshan cohort. Tregs have a strong positive correlation with tumoral PAK1 expression. (C) The mRNA levels of FOXP3 with different PAK1 expression groups are compared based on the KIRC cohort. (D-F) Quantification by flow cytometry of immune cells in ccRCC tissue samples from FCS cohort. (D) FOXP3+CD25+ CD4+ T cells frequencies of CD4+ T cells from ccRCC tissue and para-ccRCC tissue are compared by paired t-test. (E) FOXP3+CD25+ CD4+ T cells frequencies of CD4+ T cells from patients with PAK1-low (n=15) or PAK1-high tumors (n=15) are compared. (F) CD8/Treg ratio was compared in FCS cohort and Zhongshan cohort, respectively. PAK1high tumors are correlated with significantly decreased CD8/Treg ratio. (G) Volcano plot shows differentially expressed genes in high CD8/Treg ratio tumors relative to low CD8/Treg ratio tumors. mRNA levels with a $P<0.05$ and $logFC \geq 0.5$ or ≤ -0.5 are deemed differentially expressed. (H) Protein-protein interaction networks of the top 100 down-regulated genes in tumors with low CD8/Treg ratio (node degree≥7). The node size indicates node degree. The top 12 genes (node degree≥13) were highlighted in right circle. Bar plots show mean ± SEM. *p<0.05, **p<0.01, ***p<0.001 and ****p<0.0001 for groups connected by horizontal lines.

Figure 3

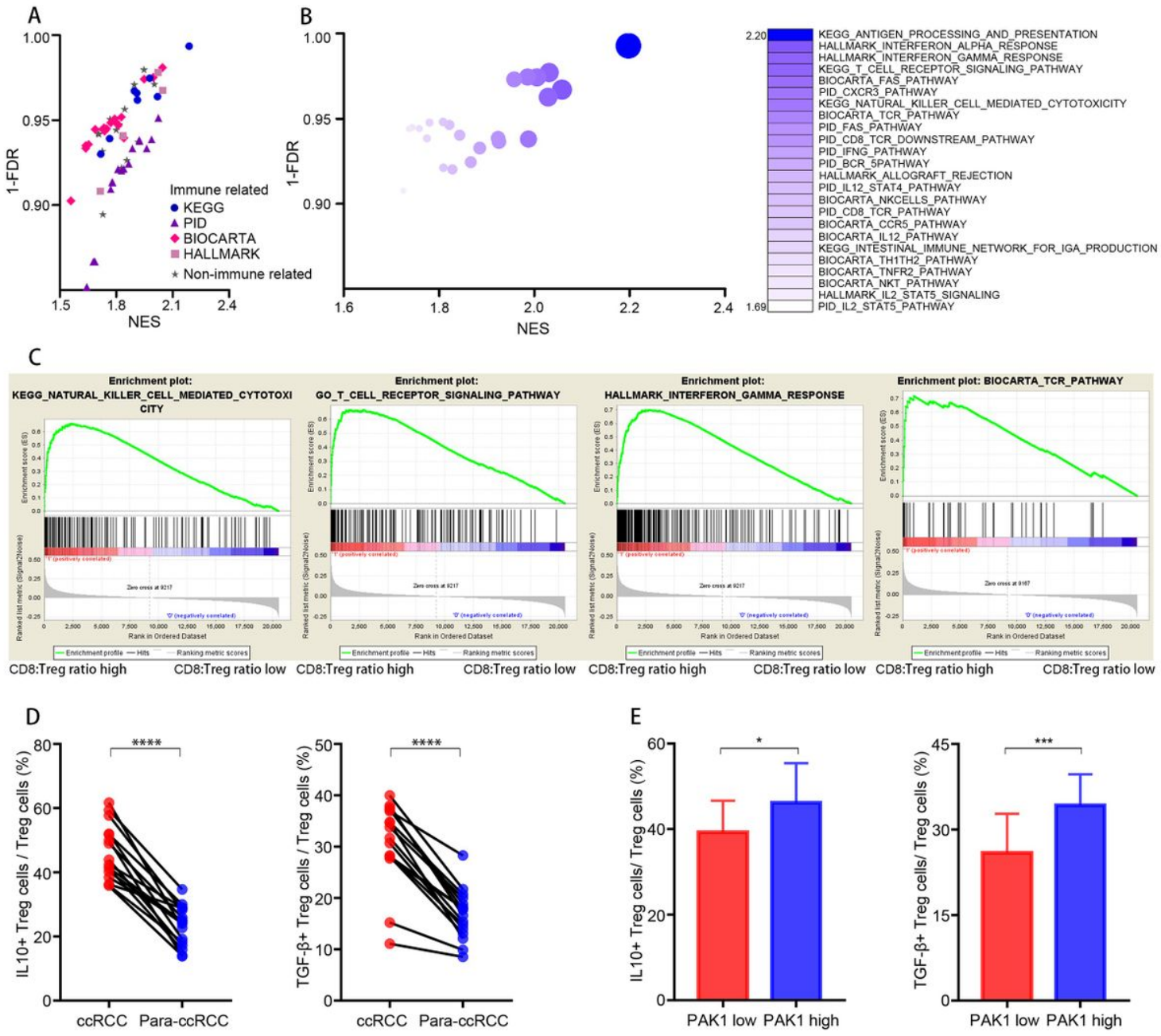

Figure 3

IL-10+ and TGF-β+ Tregs dominate immunosuppression in PAK1high ccRCC tissue. (A) GSEA (HALLMARK, KEGG, BIOCARTA and PID) pathway distribution for tumors with high CD8/Treg ratio versus tumors with low CD8/Treg ratio. (B-C) Top 24 immune-related gene sets down-regulated in tumors with low CD8/Treg ratio. (D-E) Quantification by flow cytometry of Tregs in FCS cohort. (D) IL-10+ and TGF-β+ Tregs frequencies of Tregs from ccRCC tissue or para-ccRCC tissue are compared, respectively. (E) IL-10+ and TGF-β+ Tregs frequencies of Tregs from patients with PAK1low or PAK1high tumors are compared, respectively. Bar plots show mean ± SEM. *p<0.05, **p<0.01, ***p<0.001 and ****p<0.0001 for groups connected by horizontal lines.

Figure 4

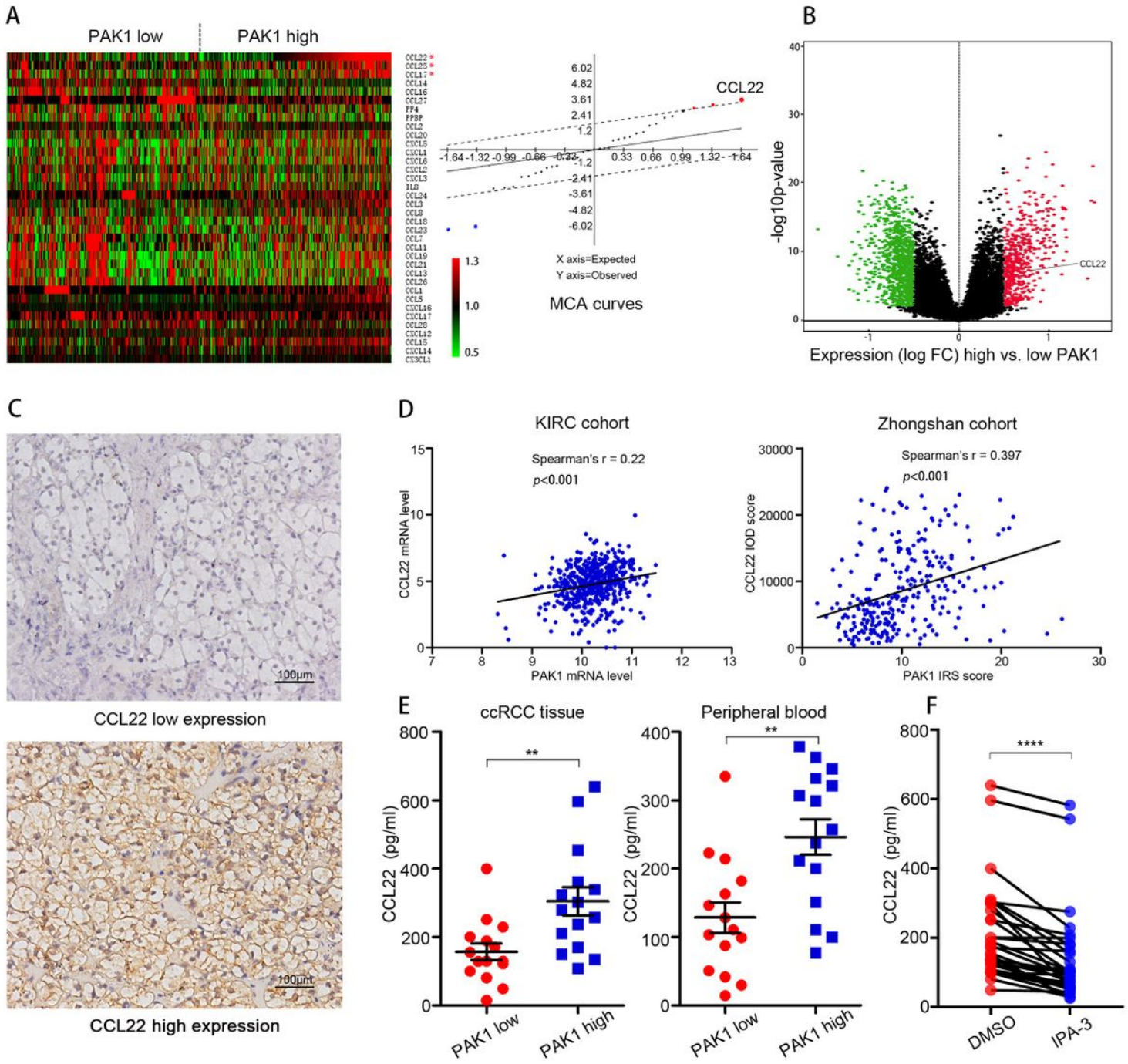

Figure 4

Increased tumoral PAK1 induces CCL22 secretion in ccRCC tissue. (A) Heatmap of relative mRNA levels of 36 common chemokines in 534 ccRCC patients based on KIRC cohort. Significance Analysis for Microarray of cytokines in heatmaps showed that CCL22 is of most significance. (B) Volcano plot shows differentially expressed genes in PAK1-high tumors relative to PAK1-low tumors. mRNA levels with a P<0.05 and logFC≥0.5 or ≤ -0.5 are deemed differentially expressed. (C) Low and high CCL22 expression in ccRCC tissue by IHC in Zhongshan cohort. Scale bar: 50 μm. (D) Correlations assessed by Spearman correlation between CCL22 and PAK1 expression by IHC in Zhongshan cohort and KIRC cohort,

respectively. (E) Quantification by ELISA of CCL22 concentrations in ccRCC tissue and peripheral blood from patients with PAK1-low (n=15) or PAK1-high tumors (n=15) are compared, respectively. (F) CCL22 concentration in ccRCC tissue samples from FCS cohort after treated with IPA-3 or DMSO (n=30). The difference between two groups is compared by paired t-test. Bar plots show mean ± SEM. *p<0.05, **p<0.01, ***p<0.001 and ****p<0.0001 for groups connected by horizontal lines.

Figure 5

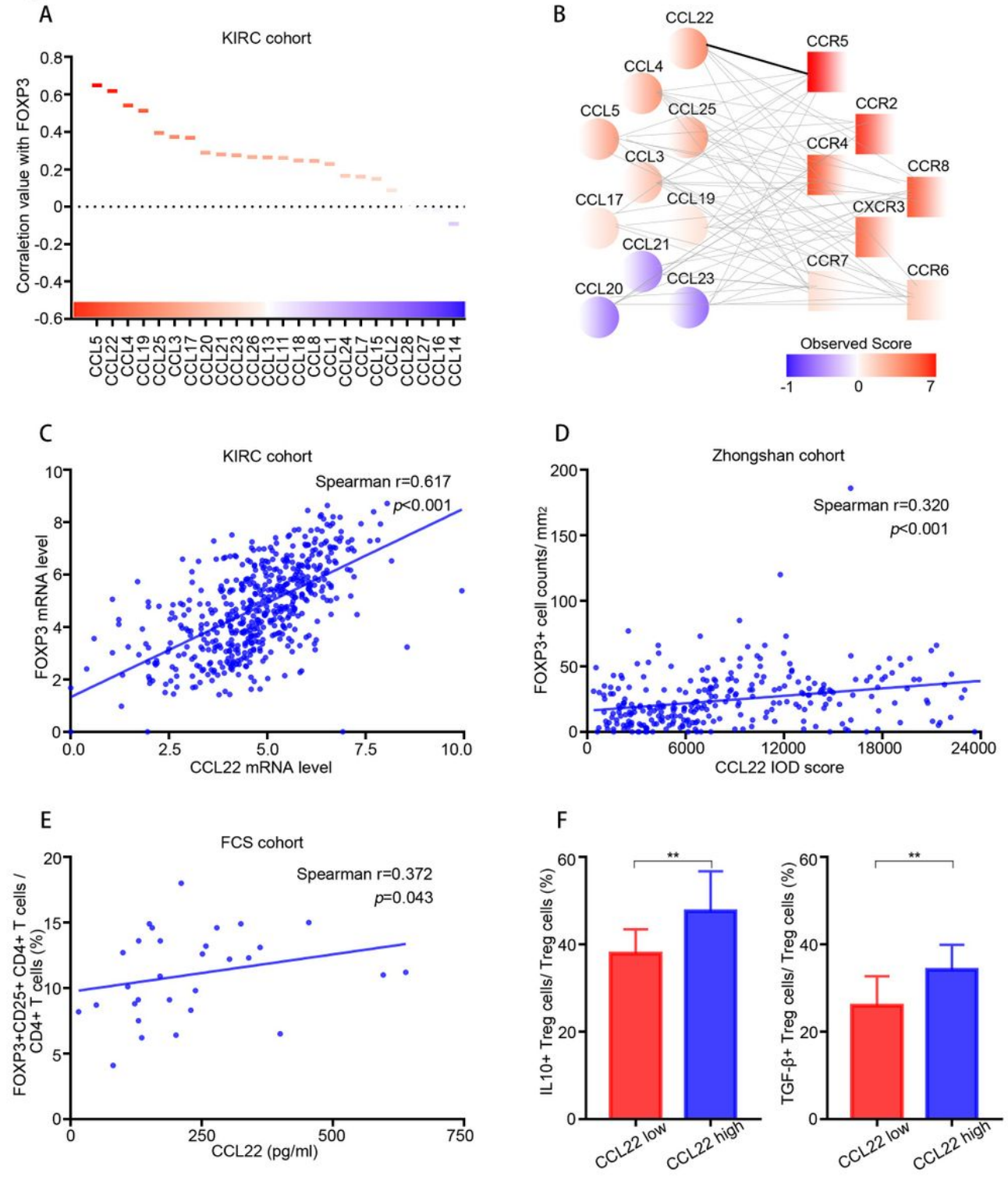

Figure 5

CCL22 promotes immunosuppression by recruiting IL-10+ and TGF-β+ Tregs in ccRCC patients. (A) Waterfall chart of Spearman correlation between FOXP3 and 24 C-C motif chemokines based on KIRC cohort. Red indicates strong positive correlations, blue indicates strong negative correlations. (B) Interaction network analysis of chemokine ligand gene expression corresponding receptor gene expression detected in PAK1high versus PAK1low tumors. Genes are ordered vertically by observed score. Lines connect interactive pairs. (C) Correlations assessed by Spearman correlation between CCL22 and FOXP3 mRNA levels in KIRC cohort. (D) Correlations assessed by Spearman correlation between CCL22 and FOXP3 expression by IHC in Zhongshan cohort. (E) Correlations assessed by Spearman correlation between CCL22 concentration and Tregs frequencies of CD4+ T cells by flow cytometry in FCS cohort. (F) IL-10+ and TGF-β+ Tregs frequencies of Tregs from patients with CCL22low (n=15) or CCL22high tumors (n=15) are compared, respectively. Bar plots show mean ± SEM. *p<0.05, **p<0.01 and ***p<0.001 for groups connected by horizontal lines.

Figure 6

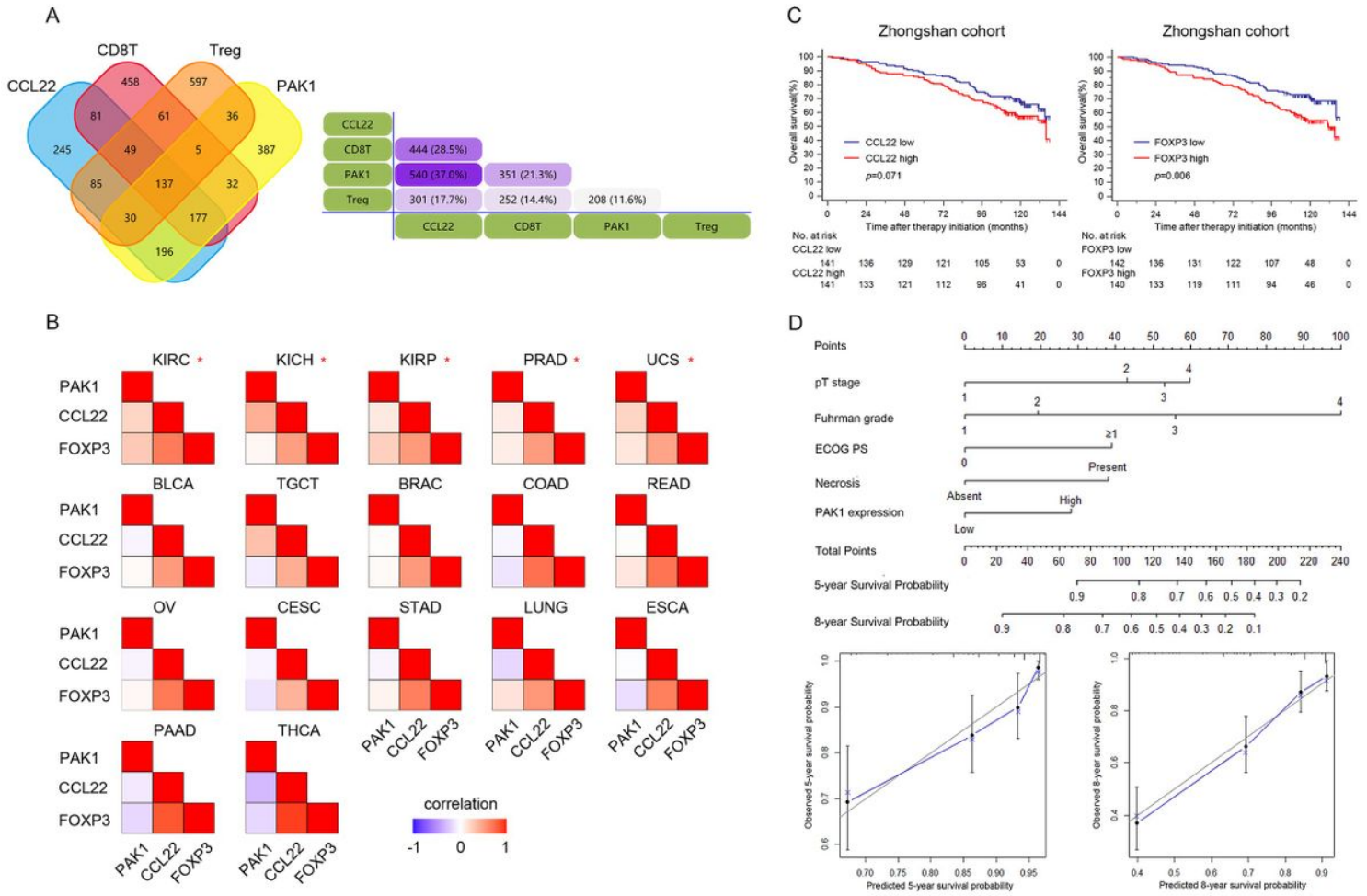

Figure 6

PAK1-CCL22-Tregs axis interlinks prognosis of ccRCC patients. (A) VENN diagram is built by top 1000 differentially expressed genes of each between-groups based on PAK1, CCL22, FOXP3 and CD8 grouping in KIRC cohort. It shows the consistency of PAK1-CCL22-Treg cell axis. Differentially expressed genes are

calculated by R software. (B) Correlation between PAK1, CCL22 and FOXP3 among 17 cancers in TCGA cohorts, * indicated significant correlations. (C) Kaplan-Meier curves comparing OS in ccRCC patients with high and low CCL22 and FOXP3 expression from Zhongshan cohort. (D) A PAK1-based nomogram is built to predict OS at 5- and 8- years after nephrectomy for ccRCC patients. The calibration plots for predicting OS at 5-years and 8-years present good consistency between actual observation and the prediction by nomogram.

Supplementary Files

This is a list of supplementary files associated with this preprint. Click to download.

- TableS2.pdf
- FigureS1.tif
- TableS1.pdf
- TableS3.pdf